COMMUNICATION

ADVANCED
OPTICAL
MATERIALS
www.advopticalmat.de

Check for
updates

Direct Observation of Shallow Trap States in Thermal Equilibrium with Band-Edge Excitons in Strongly Confined CsPbBr₃ Perovskite Nanoplatelets

Etienne Socie, Brener R. C. Vale, Andrés Burgos-Caminal, and Jacques-E. Moser*

Lead halide perovskites exhibit great potential for light-emitting devices. Enhanced photoluminescence (PL) is obtained in perovskite materials of reduced dimensionalities due to the large exciton binding energy. However, as the nanocrystal size is reduced, the surface-to-volume ratio increases, leading to an abundance of surface defects. Here, a fast PL decay, 3–10 ps, is observed in quasi-1D CsPbBr₃ perovskite nanoplatelets using broadband fluorescence upconversion spectroscopy. This decay is attributed to reversible trapping of band-edge excitons into dark states that lie close to the band edge. A simplified model is proposed to further confirm the presence of shallow traps and to fit the data obtained by ultrafast spectroscopy for multiple samples. Finally, the presence of deep trap states in aged nanoplatelets is revealed, likely arising from desorption of the organic capping ligands from the surface. Exciton trapping into these states is slower, 20–30 ps, but leads to a decrease in the photoluminescence quantum yield. These results may not only explain the extended luminescence lifetimes that have been reported for perovskite nanocrystals but also demonstrate the potential of combining ultrafast transient absorption and fluorescence up-conversion to obtain a full description of the spectroscopic properties of the material.

Lead halide perovskites are promising materials in the field of photovoltaics: in less than 10 years, their power-conversion efficiency has surpassed that of silicon solar cells, currently reaching 25.2%.[1] Such amazing results are explained by the extended carrier lifetime, long carrier diffusion lengths, and

E. Socie, B. R. C. Vale, Dr. A. Burgos-Caminal, Prof. J.-E. Moser
Photochemical Dynamics Group
Institute of Chemical Sciences & Engineering, and Lausanne
Centre for Ultrafast Science (LACUS)
École polytechnique fédérale de Lausanne
Lausanne 1015, Switzerland
E-mail: je.moser@epfl.ch
B. R. C. Vale
Grupo de Pesquisa Química de Materiais
Departamento de Ciências Naturais
Universidade Federal de São João Del-Rei
Campus Dom Bosco, São João Del-Rei, Del Rei 36301-160, Brazil

The ORCID identification number(s) for the author(s) of this article can be found under https://doi.org/10.1002/adom.202001308.

low trap state density of perovskites. Confinement of the bulk 3D structure into materials of reduced dimensionalities, such as nanoplatelets (NPls) (2D), nanorods (1D) or quantum dots (0D), has also widened the range of applications to photodetection,[2–4] lasing,[5] and light-emitting devices.[6–8] Compared to their bulk counterparts, perovskite nanocrystals (PNCs) offer greatly enhanced photoluminescence (PL) due to the strong electron–hole interaction, that is, large exciton binding energy,[9] induced by quantum confinement. One of the key features that has been ascribed to PNCs for efficient optoelectronic devices is their defect tolerance.[10,11] Indeed, the majority of the intrinsic defects in hybrid lead halide perovskites have been considered to be shallow trap states, with energies close to or within the energy bands.[12] Therefore, PNCs do not require postprocessing surface passivation, as conventional quantum dots do, to obtain high photoluminescence quantum yields (PLQYs).[13,14] Although most of the studies focused their attention on large, weakly confined, cubic PNCs,[15] the size of the PNCs could be further reduced to match the strong quantum confinement conditions (at least one dimension smaller than the exciton Bohr radius). In this case, the surface-to-volume ratio greatly increases, leading to an abundance of surface defects. In PNCs, surface defects are usually passivated by the use of organic capping ligands during synthesis.[16,17] The ligands play a role not only in the PNC PLQYs but also in their sensitivity to moisture and oxygen.[18,19] However, ligand binding to the surface is highly dynamic, which could lead to rapid desorption of the capping ligands, resulting in the formation of undercoordinated lead atoms, which act as surface traps.[20–25] Some reports have already shown that postsynthetic thiocyanate surface treatment[26,27] or inorganic passivation via the addition of ZnBr₂[28] enables efficient trap suppression and a PLQY near unity.

Since the PL tracks only the excited state population, following its dynamics is one of the easiest ways to understand the processes occurring in PNCs. However, standard techniques, such as time-correlated single-photon counting (TCSPC), have a limited time resolution of, at best, a few tens of picoseconds,[29] while exciton trapping usually occurs within the first ps after photoexcitation.[27,30] Therefore, femtosecond broadband fluorescence upconversion spectroscopy (FLUPS) is

ADVANCED
SCIENCE NEWS
www.advancedsciencenews.com

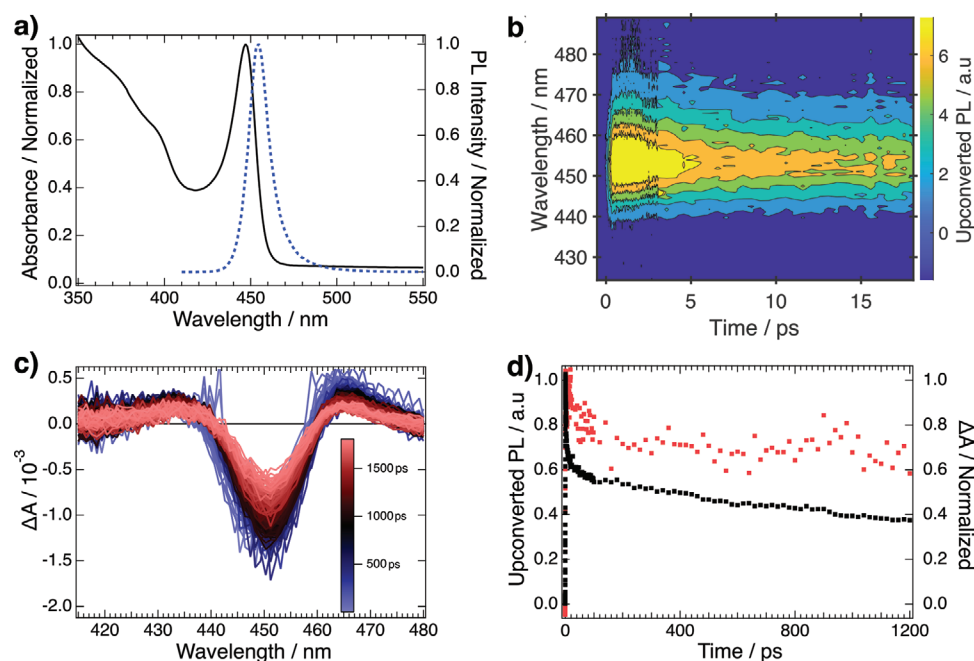ADVANCED
OPTICAL
MATERIALS
www.advopticalmat.de

Figure 1. a) Emission (blue dashed line) and absorption (black line) spectra of CsPbBr$_3$ nanoplatelets dispersed in dodecane. b) 2D time-resolved emission spectra of CsPbBr$_3$ acquired by FLUPS ($\lambda_{exc} = 400$ nm) for $<N_{ex}> = 0.2$. c) TA spectra at different time delays for $<N_{ex}> = 0.2$. d) Normalized decays of the exciton bleaching peak ($\lambda = 450$ nm) in the TA spectra (red dots) and of the fluorescence peak ($\lambda = 455$ nm) in the FLUPS spectra (black dots).

an ideal candidate for detecting the emission of PNCs. Here, the fluorescence is gated by an ultrashort laser pulse, and the complete spectrum is recorded for every fixed delay in single-scan pump-gate measurements.[31] The sub-ps time resolution of FLUPS enables a deeper understanding of the recombination mechanism occurring in PNCs. In this study, we show direct observation of shallow trap states in thermal equilibrium with the band-edge excited states in strongly confined NPls. Trapping of the photoexcited excitons results in a fast PL decay within a few ps, which does not follow the trend observed by ultrafast transient absorption spectroscopy (TAS). Moreover, we propose a model for explaining the data obtained by both FLUPS and TAS for multiple samples. Finally, we monitor the effect of sample aging on the PL dynamics and reveal the formation of deep traps in old NPl samples, resulting plausibly from ligand desorption from the surface.

Strongly confined CsPbBr$_3$ NPls were synthesized at room temperature following a procedure described elsewhere.[32] The details of the procedure are reported in the Supporting Information. **Figure 1**a shows the linear absorption and emission spectra for the as-synthesized NPls dispersed in dodecane. The absorption spectrum exhibits an intense and sharp excitonic peak at 445 nm (2.79 eV), which is a signature of strong quantum confinement. This is supported by the large 80 nm (425 meV) blueshift compared to the band-edge absorption of bulk CsPbBr$_3$ situated at 525 nm (2.36 eV).[33] As mentioned previously, the shape of the NPls is close to nanorods with dimensions of $3 \times 4 \times 23$ nm^3.[32] The PL signal is centered at 455 nm, indicating that the synthesis produced NPls of a narrow size and shape distribution. The second derivative of the absorption spectrum (Figure S1, Supporting Information) does not show negative peaks at lower energy than the first exciton transition, which further confirms the narrow size

distribution in the ensemble (see Supporting Information for details).

2D time-resolved emission spectra of the CsPbBr$_3$ NPls recorded by FLUPS are shown in Figure 1b. Here, the excitation energy fluence was set to generate an average density of $<N_{ex}> = 0.2$ excitons per particle and avoid any contribution from exciton–exciton interactions, such as Auger recombination or biexciton emission.[32,34,35] We have shown recently that the emission spectrum is very sensitive to the exciton–exciton interaction due to biexciton emission in CsPbBr$_3$ NPls. This emission is red-shifted compared to the main peak and decays over 10 ps.[32] By examining the emission slices at different time delays (Figure S2, Supporting Information), we verify the absence of multiexciton emission or energy transfer from smaller to larger particles. Indeed, the PL peak at 455 nm does not shift or sharpen over time, indicating that the emission comes from a unique population set. The transient absorption spectra (Figure 1c) show a negative signal corresponding to exciton bleaching at 450 nm. This negative response is related to the filling of the band-edge exciton and is close to the excitonic peak in the absorption spectrum. Moreover, two excited state absorption peaks are observed, one close to 470 nm corresponding to the exciton Stark effect from interactions between hot and band-edge excitons[32,36] and a broadband one on the blue side of the spectrum (<440 nm), which has been assigned to the forbidden exciton transition in strongly quantum-confined nanocrystals.[32,37] However, for bulk perovskites, this signal comes from band gap renormalization.[38]

The dynamics of the PL peak at 455 nm and of the exciton bleaching at 450 nm are normalized and compared in Figure 1d. Both exhibit a long decay component (>2 ns), which is attributed to the radiative recombination of band-edge excitons. Interestingly, while the decay of the exciton bleaching peak is mostly mono-exponential, the PL dynamics also exhibit
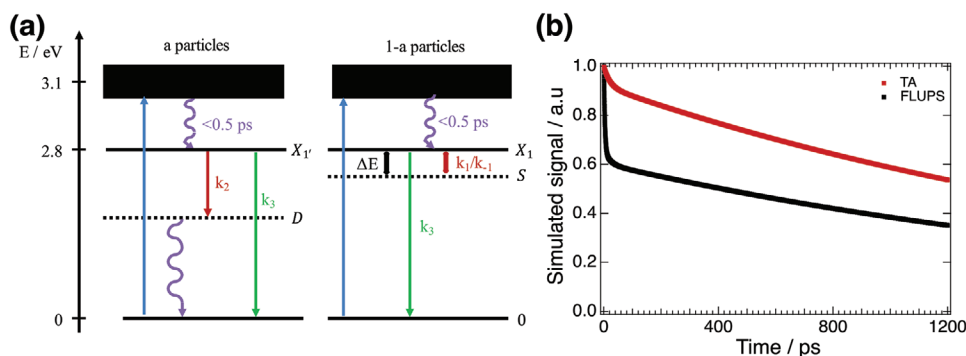
Figure 2. a) Energy diagrams illustrating the model proposed in Equations (2)–(4). On the left, energy diagram of NPls having deep trap states (D) and on the right, energy diagram of NPls having shallow trap states (S) only. On both sides, the ground and lowest excited states are denoted 0 and X_1, respectively. The black band indicates the energy of upper excited states populated after excitation by a 400 nm pump pulse (blue arrow). ΔE is the small energy difference between the shallow trap states and the lowest excited state. k_1, k_{-1}, k_2, and k_3 are the rate constants for respectively trapping into the shallow trap states, detrapping from the shallow trap states, trapping into the deep trap states, and radiative recombination. Nonradiative processes are expressed by purple wavy arrows. b) Simulated signal intensities obtained by analytically solving the proposed model for TAS (red line) and FLUPS (black line).

a short decay component of a few ps (Figure S3, Supporting Information). Knowing that the PL signal intensity depends only on the emissive state population, we presume that the fast decay is induced by a transfer from the band-edge state to dark trap states. Moreover, considering that these dark trap states are only a few meV from the band edge (shallow), they cannot be distinguished spectrally. Thus, time-resolved PL becomes crucial for probing only the emissive states.

To explain the aforementioned early dynamics, we propose a model for an ensemble of uncorrelated excitons in strongly confined perovskite NPls at a low fluence (**Figure 2**a). This model has already been reported by Chirvony et al. to explain the formation of long-lived PL kinetics in PNCs.[39,40] Second, we consider that the shallow trap states, S, and the lowest excited state, X_1, are in thermal equilibrium and the population distribution between these two states follows a Maxwell–Boltzmann distribution. Furthermore, since the energy difference between S and X_1 is considered to be less than the thermal energy $k_B T$, the trapping into the shallow trap states is reversible, and the back transfer rate constant, k_{-1}, is related to that of the trapping process, k_1, via Equation (1).

$$k_1 = k_{-1} \times e^{-\Delta E/k_B T} \tag{1}$$

$$\frac{dN_{X_1}}{dt} = -k_3 N_{X_1} - k_1 N_{X_1} + k_{-1} N_{X_S} \tag{2}$$

$$\frac{dN_{X_S}}{dt} = k_1 N_{X_1} - k_{-1} N_{X_S} \tag{3}$$

$$\frac{dN_{X_{1'}}}{dt} = -k_3 N_{X_{1'}} - k_2 N_{X_{1'}} \tag{4}$$

$$\text{Sig}_{FLUPS} = N_{X_1} + N_{X_{1'}} \tag{5}$$

$$\text{Sig}_{TA} = N_{X_1} + N_{X_{1'}} + N_{X_S} \tag{6}$$

The evolution of the population of each state after a time delay $t = 0.5$ ps is expressed in Equations (2)–(4). In such a system,

the relaxation of hot excitons has already been reported to be fast at low fluence (<0.3 ps).[32,34,36] We postulate that at time $t = 0.5$ ps, all the photoexcited excitons have relaxed to the lowest excited state. Therefore, the initial population of the lowest excited state is set at 1 and the population of the shallow states is set at 0, which corresponds to the populations of excitons that can or cannot be trapped in deep trap states and excitons trapped in shallow states, respectively. Second, to fit the data well, we need to consider two sub-ensembles, as has already been expressed by Bohn et al.[30] On the one hand, a proportion a of particles, called X_1', have deep trap states, D. The decay of the photoexcited excitons located in these particles can be radiative or trap-assisted. To simplify the differential equations and obtain analytical solutions, we neglected the contribution of shallow trap states for this subpopulation. Since the trapping rate constants k_1 and k_2 are one order of magnitude apart, the obtained trend should not be affected by this simplification but k_2 could be overestimated. On the other hand, a total of $1 - a$ excitons, called X_1 in the differential equations, cannot be trapped in D and can only decay to the ground state radiatively. The emission can be delayed by the trapping into the S-states which is reversible. The number a is proportional to the number of NPls with ligands desorbed from their surface.[23–25,41,42] The FLUPS signal intensity is only proportional to X_1 and X_1' population while the GSB intensity in TA follows the population of X_1, X_1', and S since these states are close by in energy (Equations (5) and (6)). Deep traps states are usually located in the middle of the band gap and do not contribute to the GSB signal in TA, leading to a bi-exponential decay behavior for the GSB, where the fastest decay lifetime is associated with the unreversible trapping into the D-state and the longest lifetime corresponds to the radiative recombination of band-edge excitons. However, a basic multi-exponential decay cannot be used to fit the FLUPS signal since the trapping from X_1' into the S-state is reversible, as expressed in Equation (2). Simulations, obtained by analytically solving Equations (2)–(4), are shown in Figure 2b and follow the trend observed during the measurements.

We fitted the previous model to three different samples to extract the rate constants, k_1, k_{-1}, k_2, and k_3, the small energy

ADVANCED
SCIENCE NEWS
www.advancedsciencenews.com

ADVANCED
OPTICAL
MATERIALS
www.advopticalmat.de

difference between the shallow trap states and the lowest excited state, ΔE, and the proportion of particles with deep trap states for each one. The first two samples were synthesized with different organic capping ligands: common oleic acid, referred to as NPls−OA, and trioctylphosphine, referred to as NPls−TOP, which has already been used for improving the stability of $CsPbBr_3$ NCs.[43,44] For the last sample, $ZnBr_2$ salt was added during the synthesis of NPls–OA to bring an excess of bromide, and this sample is referred to as NPls−Br. The fitted data and extracted parameters are reported in Figure S4 and Table S1, Supporting Information. The rate constants all lie in the same range for the three samples: $k_1 = 1-3 \times 10^{11}$ s^{-1}, $k_2 = 3-5 \times 10^{10}$ s^{-1}, and $k_3 = 7-8 \times 10^8$ s^{-1}, corresponding to $\tau_S = 3-10$ ps, $\tau_D = 20-30$ ps, and $\tau_{rad} = 1.2-1.4$ ns for the shallow trapping, deep trapping, and radiative recombination lifetimes, respectively. The radiative recombination rate corroborates the previous values reported in the literature,[39,45,46] and the two trapping rates are also within the range expected based on numerous studies.[30,39,40] These findings indicate that trapping into the shallow trap states is relatively fast and can fully explain the difference observed between the TA and FLUPS signals. Second, the energy difference ΔE between S and X_1 states is small ($<k_B T$), as expected. The depth of the shallow trap states depends on the passivating ligand used during the synthesis, which has already been reported.[39] Note that these states can be located slightly below or above the lowest excited state. The latter are called intra-band states and can also be active for hot carrier trapping. Finally, the proportion a of particles with deep trap states is reduced from 0.2 for NPls−OA and NPls−TOP to 0.05 for NPls−Br. This noticeable difference between the samples has already been shown in the literature.[28] Park et al. argued that an excess of Br on the surface can passivate the deep trap states and stabilize NPls. We also recorded the PL decay on longer timescale by using TCSPC. Figure S5, Supporting Information shows the dynamics on the ns range. As already observed by Vonk et al.,[47] the PL decay is multiexponential ($\tau_1 = 5$ ns and $\tau_2 = 13$ ns) due to the NPl subpopulations in the ensemble. Moreover, the bi-exponential function cannot fit the decay curve on long time scales (>100 ns). This kinetic component has already been ascribed as a delayed PL induced by the trapping and detrapping of excitons from shallow trap states.[47]

Focusing on NPls−Br, we monitored the effect of sample aging on the PL dynamics. **Figure 3**a,b shows that the linear optical properties remain unaffected after 80 days under light and room temperature. Furthermore, the second derivative of the absorption spectrum (Figure S1, Supporting Information) confirms the absence of larger particles. The small 5 nm shift observed in both the absorption and emission spectra is attributed to small growth of the NPls in the nonconfined dimension. However, the PL dynamics considerably evolve over time (Figure 3c). While the rate constant of trapping into the shallow traps, k_1, and that associated with radiative recombination of band-edge excitons, k_3, are unchanged, an intermediate PL decay of a few tens of ps appears for aged samples. We previously attributed this decay to exciton trapping into deep trap states, with the associated rate constant k_2. To investigate this observation, we fitted the data with the aforementioned model. The rate constants k_1, k_2, and k_3 and ΔE were set constant for every sample, and only the proportion a of particles with deep trap states was variable. The fits and extracted parameters are shown in Figure S6 and Table S2, Supporting Information. The number a increases from 0.05 for fresh NPls up to 0.49 after 80 days, indicating that the number of deep traps increases over time. This could be explained by the dynamic binding between the capping ligand and the NPl surface.[20–25] Over time, ligands are removed from the surface, leaving undercoordinated Br or Pb atoms that act as deep trap states.[41,42] These deep traps reduce the proportion of excitons emitting radiatively and thus reduce the PLQY.

We have shown that for each $CsPbBr_3$ colloidal dispersion synthesized, fast trapping, $\tau_S = 3-10$ ps, of band-edge excitons into shallow states lying close to the band edge, leads to a fast photoluminescence decay. The trapping is reversible, and its rate and the difference in energy between the shallow trap states and the lowest excited state depend on the type of organic capping ligand. This may explain the extended PL lifetimes that have been reported previously in the literature.[39,40,47] Additionally, we have also demonstrated the importance of capping ligands to prevent the formation of deep trap states. Desorption of the ligand from the surface due to sample aging increases the number of deep trap states and directly influences the PLQY of the NPls. Exciton trapping into deep trap states has been estimated to have a lifetime of $\tau_D = 20-30$ ps depending on the ligand. A complete understanding of the trapping mechanism in such systems is crucial for improving device performances. In this context, FLUPS has shown promise due to its sub-ps time resolution and ability to record single-scan pump-gate measurements.
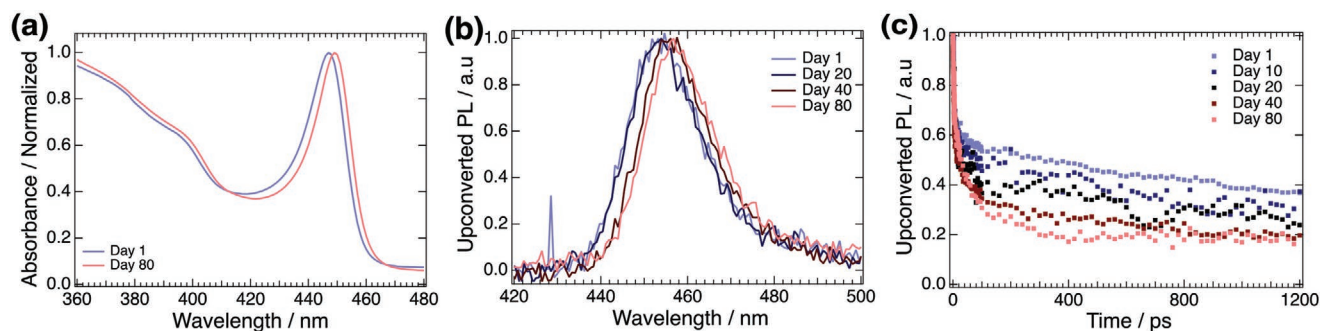

Figure 3. a) Absorption spectra of as-synthesized $CsPbBr_3$ NPls (blue line) and after 80 days (red line). b) Normalized emission spectra at $t = 1$ ps for different sample ages. c) Normalized PL decays at $\lambda_{em} = \lambda_{max}$ of the given samples.

**ADVANCED
SCIENCE NEWS**

www.advancedsciencenews.com

**ADVANCED
OPTICAL
MATERIALS**

www.advopticalmat.de

Supporting Information

Acknowledgements

Conflict of Interest

The authors declare no conflict of interest.

Keywords

[1] D. Luo, R. Su, W. Zhang, Q. Gong, *Nat. Rev. Mater.* **2020**, *5*, 44.

[2] C. H. Kang, I. Dursun, G. Liu, L. Sinatra, X. Sun, M. Kong, J. Pan, P. Maity, E.-N. Ooi, T. K. Ng, O. F. Mohammed, O. M. Bakr, B. S. Ooi, *Light: Sci. Appl.* **2019**, *8*, 94.

[3] Y.-H. Lin, W. Huang, P. Pattanasattayavong, J. Lim, R. Li, N. Sakai, J. Panidi, M. J. Hong, C. Ma, N. Wei, N. Wehbe, Z. Fei, M. Heeney, J. Labram, T. D. Anthopoulos, H. J. Snaith, *Nat. Commun.* **2019**, *10*, 4475.

[4] M. Gong, R. Sakidja, R. Goul, D. Ewing, M. Casper, A. Stramel, A. Elliot, J. Z. Wu, *ACS Nano* **2019**, *13*, 3714.

[5] J. Xu, X. Li, J. Xiong, C. Yuan, S. Semin, T. Rasing, X.-H. Bu, *Adv. Mater.* **2020**, *32*, 1806736.

[6] K. Lin, J. Xing, L. N. Quan, F. P. García de Arquer, X. Gong, J. Lu, L. Xie, W. Zhao, D. Zhang, C. Yan, W. Li, X. Liu, Y. Lu, J. Kirman, E. H. Sargent, Q. Xiong, Z. Wei, *Nature* **2018**, *562*, 245.

[7] T. Chiba, Y. Hayashi, H. Ebe, K. Hoshi, J. Sato, S. Sato, Y.-J. Pu, S. Ohisa, J. Kido, *Nat. Photonics* **2018**, *12*, 681.

[8] Y. Cao, N. Wang, H. Tian, J. Guo, Y. Wei, H. Chen, Y. Miao, W. Zou, K. Pan, Y. He, H. Cao, Y. Ke, M. Xu, Y. Wang, M. Yang, K. Du, Z. Fu, D. Kong, D. Dai, Y. Jin, G. Li, H. Li, Q. Peng, J. Wang, W. Huang, *Nature* **2018**, *562*, 249.

[9] Y. Jiang, X. Wang, A. Pan, *Adv. Mater.* **2019**, *31*, 1806671.

[10] M. V. Kovalenko, L. Protesescu, M. I. Bodnarchuk, *Science* **2017**, *358*, 745.

[11] S. ten Brinck, I. Infante, *ACS Energy Lett.* **2016**, *1*, 1266.

[12] J. Kang, L.-W. Wang, *J. Phys. Chem. Lett.* **2017**, *8*, 489.

[13] S. Gonzalez-Carrero, L. Francés-Soriano, M. González-Béjar, S. Agouram, R. E. Galian, J. Pérez-Prieto, *Small* **2016**, *12*, 5245.

[14] D. Yang, Y. Zou, P. Li, Q. Liu, L. Wu, H. Hu, Y. Xu, B. Sun, Q. Zhang, S.-T. Lee, *Nano Energy* **2018**, *47*, 235.

[15] L. Protesescu, S. Yakunin, M. I. Bodnarchuk, F. Krieg, R. Caputo, C. H. Hendon, R. X. Yang, A. Walsh, M. V. Kovalenko, *Nano Lett.* **2015**, *15*, 3692.

[16] M. C. Weidman, A. J. Goodman, W. A. Tisdale, *Chem. Mater.* **2017**, *29*, 5019.

[17] J. Shamsi, A. S. Urban, M. Imran, L. De Trizio, L. Manna, *Chem. Rev.* **2019**, *119*, 3296.

[18] M. I. Bodnarchuk, S. C. Boehme, S. ten Brinck, C. Bernasconi, Y. Shynkarenko, F. Krieg, R. Widmer, B. Aeschlimann, D. Günther, M. V. Kovalenko, I. Infante, *ACS Energy Lett.* **2019**, *4*, 63.

[19] W. Lv, L. Li, M. Xu, J. Hong, X. Tang, L. Xu, Y. Wu, R. Zhu, R. Chen, W. Huang, *Adv. Mater.* **2019**, *31*, 1900682.

[20] J. De Roo, M. Ibáñez, P. Geiregat, G. Nedelcu, W. Walravens, J. Maes, J. C. Martins, I. Van Driessche, M. V. Kovalenko, Z. Hens, *ACS Nano* **2016**, *10*, 2071.

[21] A. Pan, B. He, X. Fan, Z. Liu, J. J. Urban, A. P. Alivisatos, L. He, Y. Liu, *ACS Nano* **2016**, *10*, 7943.

[22] V. K. Ravi, P. K. Santra, N. Joshi, J. Chugh, S. K. Singh, H. Rensmo, P. Ghosh, A. Nag, *J. Phys. Chem. Lett.* **2017**, *8*, 4988.

[23] S. R. Smock, T. J. Williams, R. L. Brutchey, *Angew. Chem., Int. Ed.* **2018**, *57*, 11711.

[24] D. Yang, X. Li, H. Zeng, *Adv. Mater. Interfaces* **2018**, *5*, 1701662.

[25] D. P. Nenon, K. Pressler, J. Kang, B. A. Koscher, J. H. Olshansky, W. T. Osowiecki, M. A. Koc, L.-W. Wang, A. P. Alivisatos, *J. Am. Chem. Soc.* **2018**, *140*, 17760.

[26] B. A. Koscher, J. K. Swabeck, N. D. Bronstein, A. P. Alivisatos, *J. Am. Chem. Soc.* **2017**, *139*, 6566.

[27] S. Nakahara, H. Tahara, G. Yumoto, T. Kawawaki, M. Saruyama, R. Sato, T. Teranishi, Y. Kanemitsu, *J. Phys. Chem. C* **2018**, *122*, 22188.

[28] J. Park, Y. Kim, S. Ham, J. Y. Woo, T. Kim, S. Jeong, D. Kim, *Nanoscale* **2020**, *12*, 1563.

[29] D. Tamborini, M. Buttafava, A. Ruggeri, F. Zaooa, *IEEE Sens. J.* **2016**, *16*, 3827.

[30] B. J. Bohn, Y. Tong, M. Gramlich, M. L. Lai, M. Döblinger, K. Wang, R. L. Z. Hoye, P. Müller-Buschbaum, S. D. Stranks, A. S. Urban, L. Polavarapu, J. Feldmann, *Nano Lett.* **2018**, *18*, 5231.

[31] M. Gerecke, G. Bierhance, M. Gutmann, N. P. Ernsting, A. Rosspeintner, *Rev. Sci. Instrum.* **2016**, *87*, 053115.

[32] B. R. C. Vale, E. Socie, A. Burgos-Caminal, J. Bettini, M. A. Schiavon, J.-E. Moser, *J. Phys. Chem. Lett.* **2020**, *11*, 387.

[33] J. Butkus, P. Vashishtha, K. Chen, J. K. Gallaher, S. K. K. Prasad, D. Z. Metin, G. Laufersky, N. Gaston, J. E. Halpert, J. M. Hodgkiss, *Chem. Mater.* **2017**, *29*, 3644.

[34] N. S. Makarov, S. Guo, O. Isaienko, W. Liu, I. Robel, V. I. Klimov, *Nano Lett.* **2016**, *16*, 2349.

[35] J. A. Castaneda, G. Nagamine, E. Yassitepe, L. G. Bonato, O. Voznyy, S. Hoogland, A. F. Nogueira, E. H. Sargent, C. H. B. Cruz, L. A. Padilha, *ACS Nano* **2016**, *10*, 8603.

[36] Y. Li, R. Lai, X. Luo, X. Liu, T. Ding, X. Lu, K. Wu, *Chem. Sci.* **2019**, *10*, 5983.

[37] D. Rossi, H. Wang, Y. Dong, T. Qiao, X. Qian, D. H. Son, *ACS Nano* **2018**, *12*, 12436.

[38] Y. Yang, D. P. Ostrowski, R. M. France, K. Zhu, J. van de Lagemaat, J. M. Luther, M. C. Beard, *Nat. Photonics* **2016**, *10*, 53.

[39] V. S. Chirvony, S. González-Carrero, I. Suárez, R. E. Galian, M. Sessolo, H. J. Bolink, J. P. Martínez-Pastor, J. Pérez-Prieto, *J. Phys. Chem. C* **2017**, *121*, 13381.

[40] V. S. Chirvony, K. S. Sekerbayev, H. Pashaei Adl, I. Suárez, Y. T. Taurbayev, A. F. Gualdrón-Reyes, I. Mora-Seró, J. P. Martínez-Pastor, *J. Lumin.* **2020**, *221*, 117092.

[41] R. Grisorio, M. E. Di Clemente, E. Fanizza, I. Allegretta, D. Altamura, M. Striccoli, R. Terzano, C. Giannini, M. Irimia-Vladu, G. P. Suranna, *Nanoscale* **2019**, *11*, 986.

[42] K. Kidokoro, Y. Iso, T. Isobe, *J. Mater. Chem. C* **2019**, *7*, 8546.

[43] L. Wu, Q. Zhong, D. Yang, M. Chen, H. Hu, Q. Pan, H. Liu, M. Cao, Y. Xu, B. Sun, Q. Zhang, *Langmuir* **2017**, *33*, 12689.

[44] Y. Li, X. Wang, W. Xue, W. Wang, W. Zhu, L. Zhao, *Nano Res.* **2019**, *12*, 785.

[45] Y. Wu, C. Wei, X. Li, Y. Li, S. Qiu, W. Shen, B. Cai, Z. Sun, D. Yang, Z. Deng, H. Zeng, *ACS Energy Lett.* **2018**, *3*, 2030.

[46] Q. Li, Y. Yang, W. Que, T. Lian, *Nano Lett.* **2019**, *19*, 5620.

[47] S. J. W. Vonk, M. B. Fridriksson, S. O. M. Hinterding, M. J. J. Mangnus, T. P. van Swieten, F. C. Grozema, F. T. Rabouw, W. van der Stam, *J. Phys. Chem. C* **2020**, *124*, 8047.